SLAC–PUB–7885
ICHEP–PA08 #181
July 1998

Time Dependent $B_s^0 - \overline{B_s^0}$ Mixing Using Inclusive and Semileptonic B Decays at SLD*

The SLD Collaboration**
Stanford Linear Accelerator Center,
Stanford University, Stanford, CA 94309

Abstract

We set a preliminary 95% C.L. exclusion on the oscillation frequency of $B_s^0 - \overline{B_s^0}$ mixing using a sample of 250,000 hadronic Z^0 decays collected by the SLD experiment at the SLC between January 1996 and March 1998. The analyses determine the b-hadron flavor at production by exploiting the large forward-backward asymmetry of polarized $Z^0 \to b\overline{b}$ decays as well as information from the hemisphere opposite that of the reconstructed B decay. In one analysis, B decay vertices are reconstructed inclusively with a topological technique, and separation between B_s^0 and $\overline{B_s^0}$ decays exploits the $B_s^0 \to D_s^-$ cascade charge structure. The other analysis selects semileptonic decays reconstructed by intersecting a lepton with the trajectory of a topologically reconstructed D meson. The two analyses are combined to exclude the following values of the $B_s^0 - \overline{B_s^0}$ mixing oscillation frequency: $\Delta m_s < 1.7$ ps^{-1} and $3.3 < \Delta m_s < 5.0$ ps^{-1} at the 95% confidence level.

Paper Contributed to the XXIXth International Conference on High Energy Physics, July 23-29, 1998, Vancouver, Canada.

*Work supported in part by the Department of Energy contract DE–AC03–76SF00515.

1 Introduction

Transitions between B^0 and $\overline{B^0}$ mesons take place via second order weak interactions. In the Standard Model, a measurement of the oscillation frequency Δm_d for B_d^0–$\overline{B_d^0}$ mixing determines, in principle, the value of the Cabibbo-Kobayashi-Maskawa matrix element $|V_{td}|$, which is parameterized in terms of the Wolfenstein parameters ρ and (the CP-violating phase) η, both of which are currently poorly constrained. However, theoretical uncertainties in calculating hadronic matrix elements are large ($\sim$ 25% [1]) and thus limit the current usefulness of precise Δm_d measurements. These uncertainties are significantly reduced ($\sim$ 6–10%) for the ratio between Δm_d and Δm_s. Thus, combining measurements of the oscillation frequency of both B_d^0–$\overline{B_d^0}$ and B_s^0–$\overline{B_s^0}$ mixing translates into a measurement of the ratio $|V_{td}|/|V_{ts}|$ and provides a stronger constraint on the parameters ρ and η.

Experimentally, a measurement of the time dependence of B^0–$\overline{B^0}$ mixing requires three ingredients: (i) the B decay proper time has to be reconstructed, (ii) the B flavor at production (initial state $t = 0$) needs to be determined, as well as (iii) the B flavor at decay (final state $t = t_{\text{decay}}$). At SLD, the time dependence of B_s^0–$\overline{B_s^0}$ mixing has been studied using two different methods described below. Both methods use the same initial state flavor tag but they use different techniques to reconstruct the B decay and tag its final state flavor. The data consists of some 250,000 hadronic Z^0 decays collected with the upgrade vertex detector (VXD3) between January 1996 and March 1998. Another 150,000 hadronic Z^0 decays have been collected with the upgrade vertex detector, and they will be analyzed in a future update of this work. The analyses exploit the large longitudinal polarization of the electron beam to enhance the initial state tag. Average polarizations for the 1996 and 1997/98 running periods are (76.5±0.5)% and (73.2±0.8)%, respectively.

2 Detector, Simulation and Event Selection

Most components of the SLD detector were used in the analyses presented here. The Liquid Argon Calorimeter (LAC) was used for triggering, event shape measurement and electron identification. It provides excellent solid-angle coverage ($|\cos\theta| < 0.84$ and $0.82 < |\cos\theta| < 0.98$ in the barrel and

endcap regions, respectively). The LAC is divided longitudinally into electromagnetic and hadronic sections. The energy resolution for electromagnetic showers is measured to be $\sigma/E = 15\%/\sqrt{E(GeV)}$, whereas that for hadronic showers is estimated to be $60\%/\sqrt{E(GeV)}$. The Warm Iron Calorimeter (WIC) provides efficient muon identification for $|\cos\theta| < 0.60$. Tracking is provided by the Central Drift Chamber (CDC)[2] for charged track reconstruction and momentum measurement and the CCD pixel Vertex Detector (VXD)[3] for precise position measurements near the interaction point. These systems are immersed in the 0.6 T field of the SLD solenoid. Charged tracks reconstructed in the CDC are linked with pixel clusters in the VXD by extrapolating each track and selecting the best set of associated clusters[2]. For a typical charged particle from the primary vertex or heavy hadron decay, the total efficiency of reconstruction in the CDC and linking to VXD hits is $\sim 96\%$ within the VXD acceptance. The track impact parameter resolutions at high momenta are 11 μm and 23 μm in the $r\phi$ and rz projections respectively (z points along the beam direction), while multiple scattering contributions are $40\,\mu\text{m}\ /(p\sin^{3/2}\theta)$ in both projections (where the momentum p is expressed in GeV/c).

The centroid of the micron-sized SLC Interaction Point (IP) in the $r\phi$ plane is reconstructed with a measured precision of $\sigma_{IP} = (5 \pm 2)\,\mu$m using tracks in sets of ~ 30 sequential hadronic Z^0 decays. The median z position of tracks at their point of closest approach to the IP in the $r\phi$ plane is used to determine the z position of the Z^0 primary vertex on an event-by-event basis. A precision of $\sim 30\,\mu$m on this quantity is estimated using the $Z^0 \to b\overline{b}$ Monte Carlo (MC) simulation.

The simulated $Z^0 \to q\,\overline{q}$ events are generated using JETSET 7.4 [4]. The B meson decays are simulated using the CLEO B decay model [5] tuned to reproduce the spectra and multiplicities of charmed hadrons, pions, kaons, protons and leptons as measured at the $\Upsilon(4S)$ by ARGUS and CLEO [6]. Semileptonic decays follow the ISGW model [7] including 23% D^{**} production. The branching fractions of the charmed hadrons are tuned to the existing measurements [8]. The B mesons and b-baryons are generated with lifetimes of $\tau_{B^+} = 1.64$ ps, $\tau_{B^0} = 1.55$ ps, $\tau_{B^0_s} = 1.57$ ps, and $\tau_{\Lambda_b} = 1.22$ ps. The b-quark fragmentation follows the Peterson *et al.* parameterization [9]. Finally, the SLD detector is simulated using GEANT 3.21 [10].

Hadronic Z^0 event selection requires at least 7 CDC tracks which pass

within 5 cm of the IP in z at the point of closest approach to the beam and which have momentum transverse to the beam direction $p_\perp$ >200 MeV/c. The sum of the energy of the charged tracks passing these cuts must be greater than 18 GeV. These requirements remove background from $Z^0 \to l^+l^-$ events and two-photon interactions. In addition, the thrust axis determined from energy clusters in the calorimeter must have $|\cos\theta_T| < 0.85$, within the acceptance of the vertex detector. These requirements yield a sample of $\sim 200,000$ hadronic Z^0 decays.

Good quality tracks used for vertex finding must have a CDC hit at a radius<39 cm, and have $\geq$23 hits to insure that the lever arm provided by the CDC is appreciable. The CDC tracks must have $p_\perp$ >250 MeV/c and extrapolate to within 1 cm of the IP in $r\phi$ and within 1.5 cm in z to eliminate tracks which arise from interaction with the detector material. The fit of the track must satisfy χ^2/d.o.f.< 8. At least two good VXD links are required, and the combined CDC/VXD fit must also satisfy χ^2/d.o.f.< 8.

Both analyses make use of the inclusive topological vertexing technique [11] developed for B lifetime [12] and R_b [13] analyses to tag and reconstruct b-hadron decays. Secondary vertices are found in 65% of b hemispheres but in only 20% of c hemispheres and in less than 1% of uds hemispheres. The b purity of the sample is increased by reconstructing the vertex mass M, which includes a partial correction for missing decay products (see Ref. [2]). Requiring $M > 2$ GeV/c^2 yields a b-hadron sample with 98% b purity and 50% efficiency (for normalized decay length $> 5\sigma$). This inclusive vertexing technique has been adapted for semileptonic decays to reconstruct the D decay topology (see below).

3 Initial State Flavor Tagging

The large forward-backward asymmetry for $Z^0 \to b\,\overline{b}$ decays is used as a tag of the initial state flavor. The polarized forward-backward asymmetry $\tilde{A}_{FB}$ can be described by

$$\tilde{A}_{FB} = 2A_b \, \frac{A_e - P_e}{1 - A_e P_e} \, \frac{\cos\theta_T}{1 + \cos^2\theta_T} \ , \tag{1}$$

where $A_b = 0.94$ and $A_e = 0.150$ (Standard Model values), P_e is the electron beam longitudinal polarization, and θ_T is the angle between the thrust

axis and the electron beam direction (the thrust axis is signed such that it points in the same hemisphere as the reconstructed vertex). Thus, left-(right-)polarized electrons tag b ($\bar{b}$) quarks in the forward hemisphere, and $\bar{b}$ (b) quarks in the backward hemisphere. This yields an average correct tag probability of 0.74 for an average electron polarization $P_e = 73\%$. The probability for correctly tagging a b quark at production is expressed as

$$P_A(b) = \frac{1 + \tilde{A}_{FB}}{2} \ . \tag{2}$$

A jet charge technique is used in addition to the polarized forward-backward asymmetry. For this tag, tracks in the hemisphere opposite that of the reconstructed vertex are selected. These tracks are required to have momentum transverse to the beam axis $p_\perp > 0.15$ GeV/c, total momentum $p < 50$ GeV/c, impact parameter in the plane perpendicular to the beam axis $\delta < 2$ cm, distance between the primary vertex and the track at the point of closest approach along the beam axis $\Delta z < 10$ cm, and $|\cos\theta| < 0.87$. With these tracks, an opposite hemisphere momentum-weighted track charge is defined as

$$Q_{opp} = \sum_i q_i \left|\vec{p}_i \cdot \hat{T}\right|^\kappa \ , \tag{3}$$

where q_i is the electric charge of track i, $\vec{p}_i$ its momentum vector, $\hat{T}$ is the thrust axis direction, and κ is a coefficient chosen to be 0.5 to maximize the separation between b and $\bar{b}$ quarks. The probability for correctly tagging a b quark in the initial state of the vertex hemisphere can be parameterized as

$$P_Q(b) = \frac{1}{1 + e^{\alpha Q_{opp}}} \ , \tag{4}$$

where the coefficient $\alpha = -0.27$, as determined using the Monte Carlo simulation. This technique yields an average correct tag probability of 0.65 and is independent of the polarized forward-backward asymmetry tag.

Finally, the tag is further enhanced by the addition of other flavor-sensitive quantities from the hemisphere opposite that of the selected vertex. For this purpose, the inclusive topological vertexing technique mentioned earlier is used. The sensitive variables are: the total track charge and charge dipole of a topologically reconstructed vertex, the charge of a kaon identified in the Cherenkov Ring Imaging Detector, and the charge of a lepton with

high transverse momentum with respect to the direction of the nearest jet. The addition of these tags improves the average correct tag probability by about 0.03.

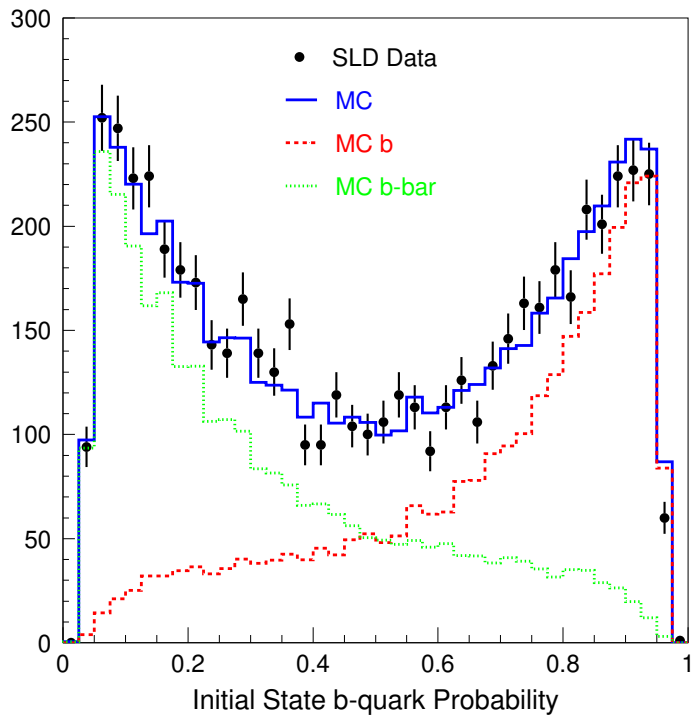

Figure 1: *Distribution of the computed initial state b-quark probability for data (points) and Monte Carlo (histograms) showing the* b *and* $\bar{b}$ *components for the events selected in the Charge Dipole analysis.*

The various tags are combined to form an overall initial state tag characterized by a b-quark probability P_i. The average correct tag probability is 0.80 with full efficiency. Fig. 1 shows the P_i distributions for data and Monte Carlo in the Charge Dipole analysis (see below for a description of the analysis), and also indicates the clear separation between b and $\overline{b}$ quarks.

4 Lepton+D Analysis

The lepton+"D" analysis aims at reconstructing the B and D vertex topologies of semileptonic B decays. It proceeds by first selecting event hemispheres

containing an identified lepton (e or μ) with $|\cos\theta| < 0.7$. Then, a D vertex candidate is reconstructed using a similar topological technique as that described earlier. This vertex is constrained to lie near the plane containing the lepton track and the IP, and to be downstream of the lepton, thereby reducing the confusion between primary and secondary tracks and thus allowing efficient reconstruction of semileptonic B decays at short decay lengths. Several cuts are added to clean up the D vertex candidate and reduce the contamination from cascade ($b \to c \to l$) charm semileptonic decays. The cuts are as follows: the lepton momentum transverse to the D trajectory $p_T > 0.9$ GeV/c, the invariant mass of all D vertex tracks (assumed to be pions) is less than 1.95 GeV/c^2 and the sum of all track charges at the D vertex is ≤ 1 in absolute value. An additional requirement aimed at suppressing the ($b \to c \to l$) contribution is that either the χ^2 for fitting the lepton and D vertex tracks to a single vertex is larger than that obtained for the D vertex tracks alone or the invariant mass of the lepton + D vertex tracks is greater than 2.5 GeV/c^2. Furthermore, the difference in the mass between the $D+l$ and the D tracks alone is greater than 0.6 GeV/c^2. The B decay vertex is reconstructed by intersecting the lepton and D trajectories. For this analysis, only vertices with positive reconstructed decay length are selected.

To enhance the fraction of B_s^0 decays, the sum of lepton + D vertex track charges is required to be $Q = 0$. This enhances the B_s^0 fraction to 15.3% of all b hadrons in the $Z^0 \to b\,\overline{b}$ MC (the B_s^0 production fraction in the $Z^0 \to b\,\overline{b}$ MC is 11.5%). Although the analysis described above achieves good b-hadron purity, an additional reduction in the non-b background is achieved at only a small cost in efficiency by applying an event b tag: the event should contain either at least one hemisphere with an inclusive topological vertex with $M > 1.6$ GeV/c^2 or a minimum of 2 tracks with positive 3-D impact parameter greater than $3\,\sigma$. As a result, the $udsc$ contamination is reduced from 9.2% to 1.9% in the final sample.

A sample of 1492 decays is thus obtained in the 1996-98 data. Various comparisons between data and Monte Carlo simulation were performed which generally showed good agreement. For example, Fig. 2 shows the distributions of lepton momentum transverse to the D vertex trajectory, D vertex track multiplicity, and invariant mass of all tracks in the D vertex and (assuming all tracks are pions) as well as in both B and D vertices.

A powerful check of the analysis and the purity of the final state tag is

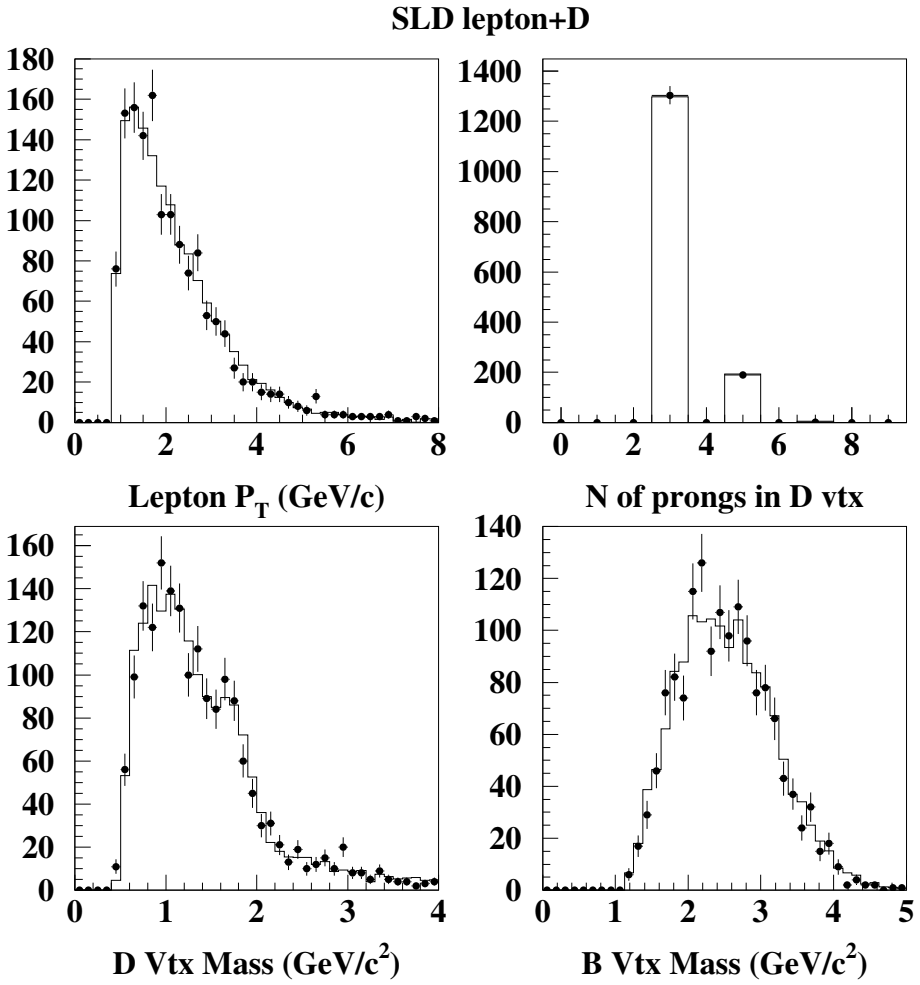

Figure 2: *Distributions of lepton momentum transverse to the D vertex trajectory, D vertex track multiplicity, D vertex mass (with the cut on the mass removed) and lepton+D vertex mass for data (points) and Monte Carlo (histograms).*

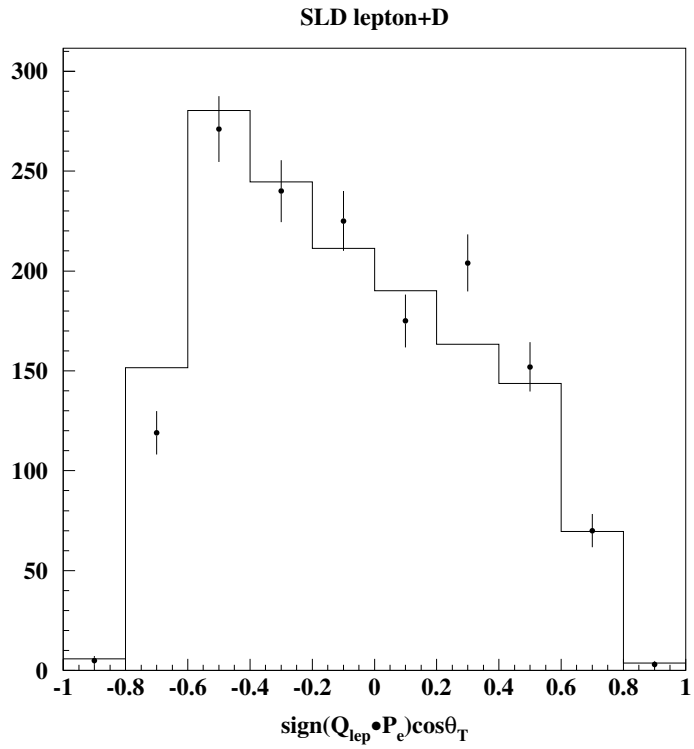

Figure 3: *Distribution of* $\cos\theta$ *for the thrust axis direction signed by the product* $(Q_{lept} \times P_e)$ *for data (points) and Monte Carlo (histograms).*

the polarization-dependent forward-backward asymmetry shown in Fig. 3. A clear asymmetry is observed, in reasonable agreement with the Monte Carlo, indicating that the final state tag purity is adequately modeled in the simulation.

The study of the time dependence of B_s^0–$\overline{B_s^0}$ mixing requires a precise determination of the B decay proper time $t = L/(\gamma\beta c)$, where L is the reconstructed decay length (distance between the IP and the B vertex) and $\gamma\beta = p_B/m_B$ is computed from the estimated B momentum p_B and the known mass of the B meson, m_B. Reconstruction of the b-hadron boost uses both tracking and calorimeter information. A detailed description of the reconstruction algorithm may be found in Ref. [14]. The overall performance of the decay length and boost measurements for B_s^0 decays proceeding via the direct $(b \to l)$ transition is shown in Fig. 4. The proper time distribution

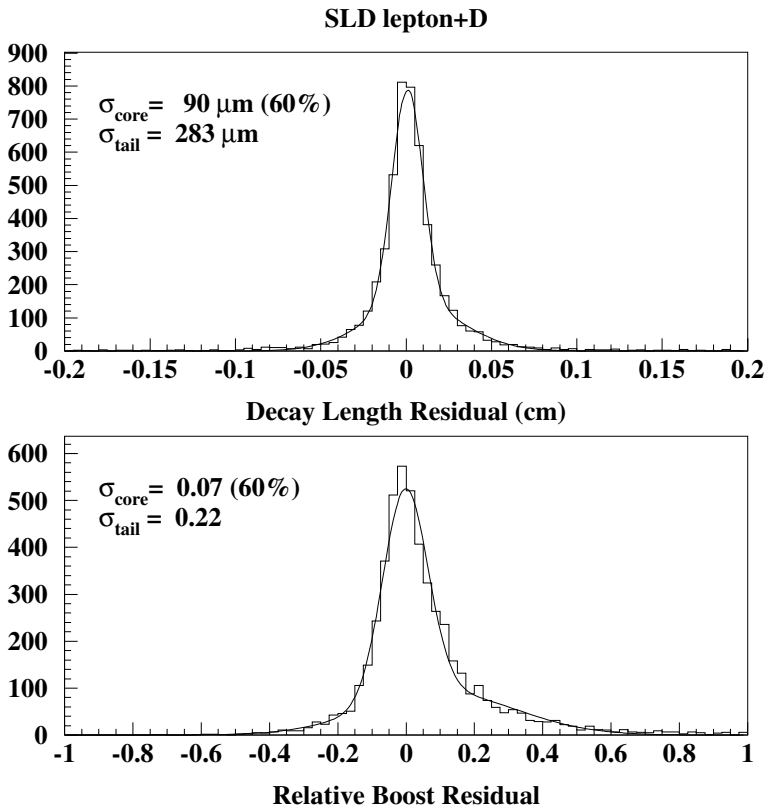

Figure 4: *Distributions of the decay length and relative boost residuals for* B_s^0 *(*$b \to l$*) decays in the simulation.*

is shown in Fig. 5.

The final state B^0 or $\overline{B^0}$ flavor is tagged by the sign of the lepton charge. Each decay is assigned a final state b-quark probability P_f, defined such that $P_f > 0.5$ (< 0.5) corresponds to a negatively (positively) charged lepton which then tags the decay as $\overline{B}$ (B). The magnitude of the correct tag probability depends on the sample composition as well as on the lepton p_T. The lepton sources in selected B_s^0 decays are as follows: 84.7% ($b \to l^-$), 6.3% ($b \to c \to l^+$), 2.2% ($b \to \bar{c} \to l^-$), 2.0% ($b \to X^-$) (right-sign misidentified lepton), 2.1% ($b \to X^+$) (wrong-sign misidentified lepton), 1.9% ($b \to$ other $\to l^-$), and 0.8% ($b \to$ other $\to l^+$). The final state correct tag probability is thus 0.908. Further enhancement of the tag is achieved by taking into account the strong p_T dependence of the various lepton source

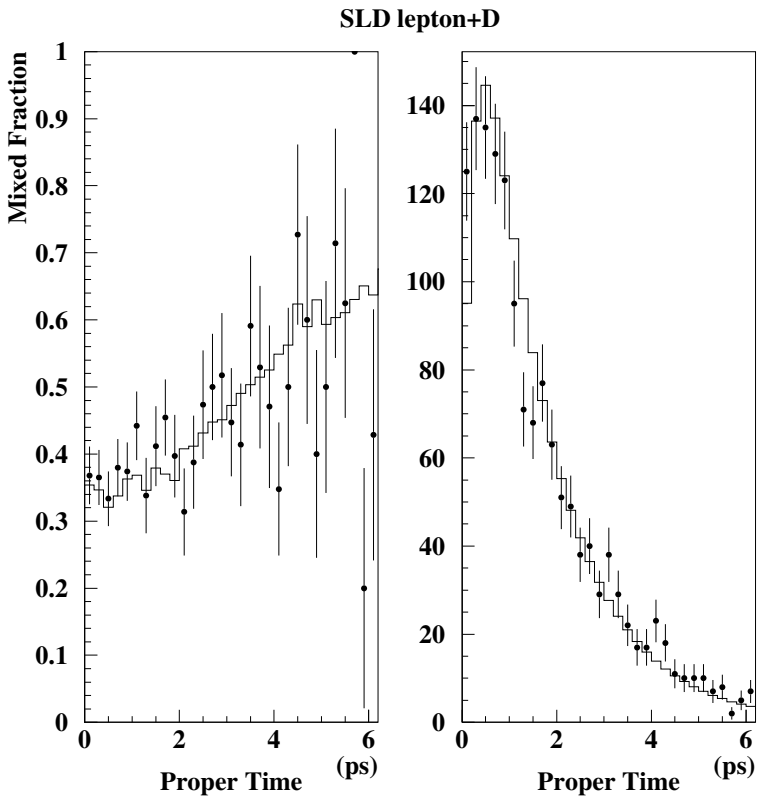

Figure 5: *Distributions of the fraction of decays tagged as "mixed" (left) and reconstructed proper time (right) for the data (points) and the likelihood function (histograms).*

fractions. At high p_T the correct tag probability for B_s^0 decays increases to 0.953.

4.1 Likelihood Analysis

The search for the time dependence of B_s^0–$\overline{B_s^0}$ mixing is carried out with a likelihood analysis which includes the effect of detector smearing, mistag of both initial and final states, selection efficiencies and the dependence on the oscillation frequency Δm_s. The probability that a meson created as a B_s^0

($\overline{B_s^0}$) will decay as a B_s^0 ($\overline{B_s^0}$) after proper time t can be written as

$$P_u(t) = \frac{\Gamma}{2}\, e^{-\Gamma t}\ [1 + \cos(\Delta m_s\, t)]\ , \tag{5}$$

where Δm_s is the mass difference between the mass eigenstates, Γ is the average decay width of the two states and P_u denotes the probability to remain 'unmixed'. The effects of CP violation are assumed to be small and are neglected. Similarly, the probability that the same initial state will 'mix' and decay as its antiparticle is

$$P_m(t) = \frac{\Gamma}{2}\, e^{-\Gamma t}\ [1 - \cos(\Delta m_s\, t)]\ . \tag{6}$$

Decays are tagged as mixed or unmixed if the product $(P_i - 0.5) \times (P_f - 0.5)$ is smaller or greater than 0, respectively. The probability for a decay to be in the mixed sample is expressed as:

$$\begin{aligned}
\mathcal{P}_{mixed}(t, \Delta m_s) \;=\;& f_u \frac{e^{-t/\tau_u}}{\tau_u}\ \eta_u \\
&+ \frac{f_d}{2} \frac{e^{-t/\tau_d}}{\tau_d} [\eta_d(1 + \cos \Delta m_d t) + (1 - \eta_d)(1 - \cos \Delta m_d t)] \\
&+ \frac{f_s}{2} \frac{e^{-t/\tau_s}}{\tau_s} [\eta_s(1 + \cos \Delta m_s t) + (1 - \eta_s)(1 - \cos \Delta m_s t)] \\
&+ f_\Lambda \frac{e^{-t/\tau_\Lambda}}{\tau_\Lambda}\ \eta_\Lambda \\
&+ \frac{f_{udsc}}{2}\ F_{udsc}(t),
\end{aligned}$$

where f_j represents the fraction of each b-hadron type and background ($j = u, d, s, \Lambda, udsc$ correspond to B^+, B_d^0, B_s^0, b-baryon, and $udsc$ background), τ_j and η_j are the lifetime and mistag probability for b hadrons of type j, and $F_{udsc}(t)$ is a function describing the proper time distribution of the $udsc$ background (a sum of two exponentials is used). A similar expression for the probability $\mathcal{P}_{unmixed}$ to observe a decay tagged as unmixed is obtained by replacing the mistag rate η by $1 - \eta$.

Detector and vertex selection effects are introduced by convoluting the above probability functions with a proper time resolution function $\mathcal{R}(T, t)$

and a time-dependent efficiency function $\varepsilon(t)$:

$$P_{mixed}(T, \Delta m_s) = \int_0^\infty \mathcal{P}_{mixed}(t, \Delta m_s)\ \mathcal{R}(T,t)\ \varepsilon(t)\ dt\ , \tag{7}$$

where t is the "true" time and T is the reconstructed time. Again, a similar expression applies to the unmixed probability $P_{unmixed}$. The resolution function is parameterized by the sum of two Gaussians:

$$\begin{aligned} \mathcal{R}(T,t) &= f_1\ \frac{1}{\sigma_1(t)\sqrt{2\pi}}\ e^{-\frac{1}{2}\left(\frac{T-t}{\sigma_1(t)}\right)^2} \\ &\quad + f_2\ \frac{1}{\sigma_2(t)\sqrt{2\pi}}\ e^{-\frac{1}{2}\left(\frac{T-t}{\sigma_2(t)}\right)^2}\ , \end{aligned}$$

where the fraction f_1 is set to 60% and $f_2 = 1 - f_1$. The proper time resolution is a function of proper time and also depends on the measured boost $\gamma\beta$, its resolution $\sigma_{\gamma\beta}$ and on the estimate of the decay length resolution σ_L:

$$\sigma(t) = \left[\left(\frac{\sigma_L}{\gamma\beta c} \right)^2 + \left(t\, \frac{\sigma_{\gamma\beta}}{\gamma\beta} \right)^2 \right]^{1/2}\ . \tag{8}$$

For each decay, the resolution σ_L is computed from the vertex fit and IP position measurement errors, with a scale factor determined using the MC simulation (the scale factor is introduced mostly to account for the fact that the analysis does not attempt to fully reconstruct the D meson decay). The relative boost residual $\sigma_{\gamma\beta}/\gamma\beta$ is parameterized as a function of the lepton + D vertex total track energy, with parameters extracted from the MC simulation. Similarly, the efficiency $\varepsilon(t)$ is parameterized using the MC simulation. All parameterizations are performed separately for each b-hadron type. For example, the efficiency for B_s^0 decays is given by

$$\varepsilon(t) = a\ \frac{1 - e^{bt}}{1 + e^{bt}} + c\ , \tag{9}$$

with $a = 0.025$, $b = -4.3$, and $c = 0.0097$. Furthermore, σ_L and $\sigma_{\gamma\beta}$ resolutions are handled separately for the main lepton sources ($b \to l$), ($b \to c(\bar{c}) \to l$) and ($b \to X$). As a consequence, different resolution functions are used for the different sources and the expressions for P_{mixed} and $P_{unmixed}$ are modified accordingly.

The study of the time dependence of B_s^0–$\overline{B_s^0}$ mixing is carried out using the amplitude method described in Ref. [15]. Instead of fitting for Δm_s directly, the analysis is performed at fixed values of Δm_s and a fit to the amplitude A of the oscillation is performed, i.e. in the expression for the mixed and unmixed probabilities, one replaces $[1 \pm \cos(\Delta m_s t)]$ with $[1 \pm A\cos(\Delta m_s t)]$. This method is similar to Fourier transform analysis and has the advantage of facilitating the combination of results from different analysis techniques and different experiments.

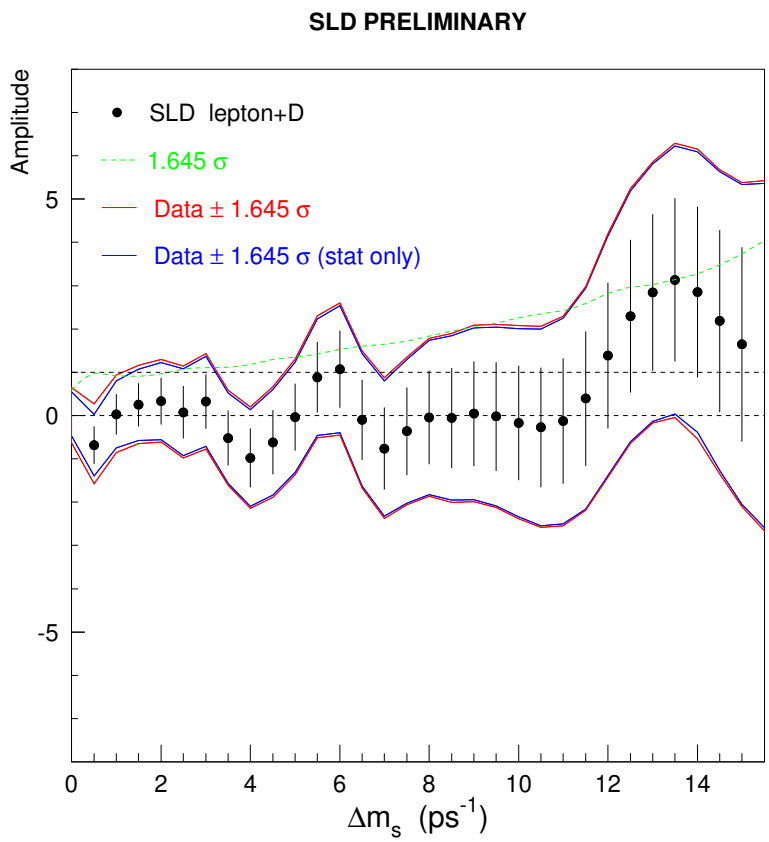

Figure 6: *Measured amplitude as a function of Δm_s in the lepton+D analysis.*

The measured amplitude for the lepton+D analysis is shown as a function of Δm_s in Fig. 6. The measured values are consistent with $A = 0$ for the whole range of Δm_s up to 15 ps^{-1} and no evidence is found for a preferred mixing frequency.

Table 1: Measured values of the oscillation amplitude A with a breakdown of systematic uncertainties for several Δm_s values in the lepton+D analysis.

Δm_s	2 ps^{-1}	5 ps^{-1}	10 ps^{-1}
Measured amplitude A	0.335	-0.038	-0.169
σ_A^{stat}	± 0.541	± 0.774	± 1.320
σ_A^{syst}	$^{+0.223}_{-0.194}$	$^{+0.273}_{-0.222}$	$^{+0.379}_{-0.216}$
$f_s = \mathcal{B}(b \to B_s^0)$	$^{-0.142}_{+0.194}$	$^{-0.181}_{+0.256}$	$^{-0.179}_{+0.250}$
$f_\Lambda = \mathcal{B}(b \to b\text{−baryon})$	$^{+0.037}_{-0.034}$	$^{+0.061}_{-0.057}$	$^{+0.047}_{-0.044}$
$udsc$ fraction	$^{+0.082}_{-0.111}$	$^{+0.052}_{-0.082}$	$^{-0.002}_{-0.034}$
decay length resolution	$^{+0.008}_{-0.005}$	$^{+0.027}_{-0.021}$	$^{+0.030}_{-0.062}$
boost resolution	$^{+0.015}_{-0.005}$	$^{-0.003}_{-0.064}$	$^{+0.242}_{+0.113}$
b-hadron lifetimes	$^{+0.006}_{-0.006}$	$^{+0.020}_{-0.021}$	$^{+0.030}_{-0.029}$
Δm_d	$^{-0.029}_{+0.023}$	$^{-0.020}_{+0.019}$	$^{+0.006}_{-0.006}$
initial state tag	$^{-0.042}_{+0.040}$	$^{+0.028}_{-0.028}$	$^{+0.076}_{-0.081}$
$\mathcal{B}(b \to l)$, $\mathcal{B}(b \to \bar{c} \to l)$, $\mathcal{B}(b \to c \to l)$	$^{+0.038}_{-0.037}$	$^{+0.015}_{-0.013}$	$^{+0.006}_{-0.004}$
lepton misidentification	$^{+0.014}_{-0.014}$	$^{+0.001}_{-0.001}$	$^{+0.005}_{-0.005}$

Systematic uncertainties have been computed following Ref. [15] and are summarized in Table 1 for several Δm_s values. Uncertainties in the sample composition are estimated by varying the fraction of $udsc$ background by $\pm 50\%$ and the production fractions of B_s^0 and b-baryons according to 0.115 ± 0.020 and 0.072 ± 0.040, respectively. Other physics modeling uncertainties are $\tau(B^+) = 1.64 \pm 0.04$ ps, $\tau(B_d^0) = 1.55 \pm 0.04$ ps, $\tau(B_s^0) = 1.57 \pm 0.06$ ps, $\tau(\Lambda_b) = 1.22 \pm 0.06$ ps, and $\Delta m_d = 0.480 \pm 0.020$ ps^{-1}. Uncertainties in the modeling of the detector include a $\pm 10\%$ variation in both decay length and boost resolutions. Initial state tag uncertainties are estimated by varying the correct tag probability by ± 0.02 (i.e., a $\pm 10\%$ variation of the mistag rate). Final state tag uncertainties include a $\pm 50\%$ variation in the lepton misidentification rate, as well as the effect of uncertainties in the branching ratios $\mathcal{B}(b \to l) = 0.112 \pm 0.002$, $\mathcal{B}(b \to \bar{c} \to l) = 0.016 \pm 0.004$, and $\mathcal{B}(b \to c \to l) = 0.080 \pm 0.004$. The dominant uncertainty is the B_s^0

production fraction in $Z^0 \to b\,\overline{b}$ events.

5 Vertex Charge Dipole Analysis

The Charge Dipole analysis aims at reconstructing the B and D vertex topologies in inclusive decays and tags the B^0 or $\overline{B^0}$ decay flavor based on the charge difference between the B and D vertices. This analysis technique is unique to SLD. Hemispheres containing an inclusive topological vertex with $M > 2$ GeV/c^2 are selected and the total vertex track charge Q is required to be 0 to enhance the fraction of B_s^0 decays in the sample and to increase the quality of the charge difference reconstruction for neutral B decays. To select decays with non-negligible separation between the B and D decay points, the probability for fitting all tracks to a single vertex is required to be less than 1%. The tracks are then rearranged into various two-vertex combinations and the combination with the lowest overall χ^2 is selected. The vertex that is closer to the IP is labelled "B" and that further away is labelled "D." MC studies indicate that the track assignment to the B (D) vertex is 66% (71%) correct. A "Charge Dipole" is defined as $\delta Q \equiv D_{BD} \times SIGN(Q_D - Q_B)$, where D_{BD} is the distance between the two vertices and Q_B (Q_D) is the charge of the B (D) vertex. Positive (negative) values of δQ tag $\overline{B^0}$ (B^0) decays and the correct tag probability increases with increasing $|\delta Q|$. Requirements on the vertices are: $200\,\mu$m $< D_{BD} <$ 1 cm, D vertex mass $<$ 1.9 GeV/c^2 (assuming all tracks are pions), B vertex decay length $L > 0$ and $Q_B \neq Q_D$. For all data and MC events, hemispheres already containing a vertex selected by the lepton+D analysis are removed such that the two analyses are statistically uncorrelated. The *udsc* background is further suppressed by demanding that the event contains either an opposite hemisphere topological vertex with $M > 1.6$ GeV/c^2 or at least 2 tracks with positive 3-D impact parameter $> 3\,\sigma$. The *udsc* fraction is thus reduced to 2.6%.

Applying all the above cuts, a sample of 5719 decays is selected in the 1996-98 data. Figure 7 shows distributions of the B and D vertex track multiplicities, and distance and charge difference between B and D vertices in the selected sample. Good agreement between data and MC is obtained. The B_s^0 fraction estimated from the $Z^0 \to b\,\overline{b}$ MC is 15.2%. Figure 8 displays the distribution of charge dipole δQ for the data sample and also indicates the separation between b hadrons containing b or $\bar{b}$ quarks in the MC.

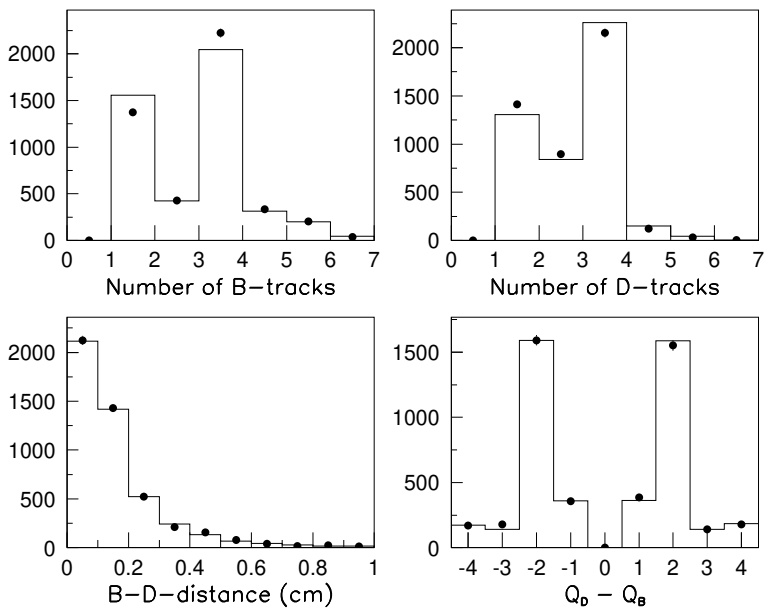

Figure 7: *Distributions of B and D vertex track multiplicity, as well as distance and charge difference between B and D vertices for data (points) and Monte Carlo (histograms) in the Charge Dipole analysis.*

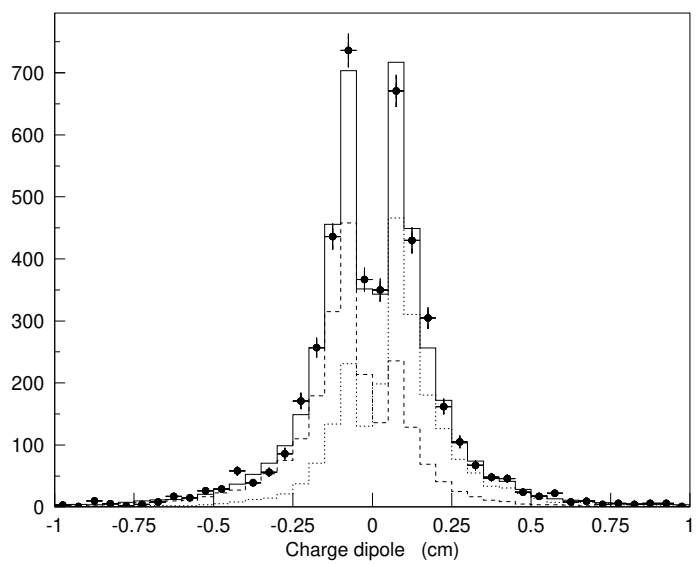

Figure 8: *Distribution of the vertex charge dipole for data (points) and Monte Carlo (solid histogram). Also shown are the contributions from b hadrons containing a b quark (dotted histogram) or a $\bar{b}$ quark (dashed histogram).*

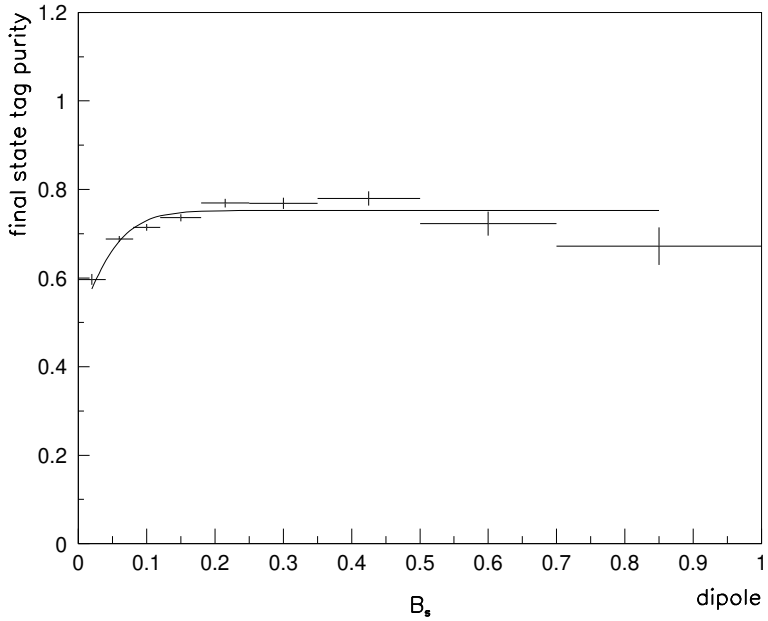

Figure 9: *Charge dipole tag purity as a function of the absolute value of the charge dipole in simulated B_s^0 decays. The function is the result of a fit.*

The average correct tag probability for the charge dipole tag is 0.69 for selected B_s^0 decays and is parameterized as a function of $|\delta Q|$, as shown in Fig. 9. Furthermore, the correct tag probability depends on the reconstructed decay length and is therefore parameterized in four different ranges: 0 – 0.5 mm, 0.5 – 1.0 mm, 1.0 – 3.0 mm, and above 3.0 mm.

As hadronic decays of B mesons are not as well known as semileptonic decays, it is important to check the tag purity estimated using measured quantities like the polarization-dependent forward-backward asymmetry shown in Fig. 10. Fair agreement with the MC is observed, indicating that the purity is reasonably modeled. It should be noted that this asymmetry is diluted by B^0–$\overline{B^0}$ mixing. Another useful test of the charge dipole tag in B_d^0 decays is the measurement of the time dependence of B_d^0–$\overline{B_d^0}$ mixing. This has been checked by fitting the fraction of decays tagged as mixed as a function of Δm_d (see Fig. 11) with a fitting technique detailed in Ref. [16]. The measured value is found to be $\Delta m_d = 0.541 \pm 0.047$ ps^{-1} (statistical error only) with a χ^2 per degree of freedom of 9.1/10. This value is in reasonable agreement with the latest world average value of 0.471 ± 0.016 ps^{-1} [17]. Fig. 11

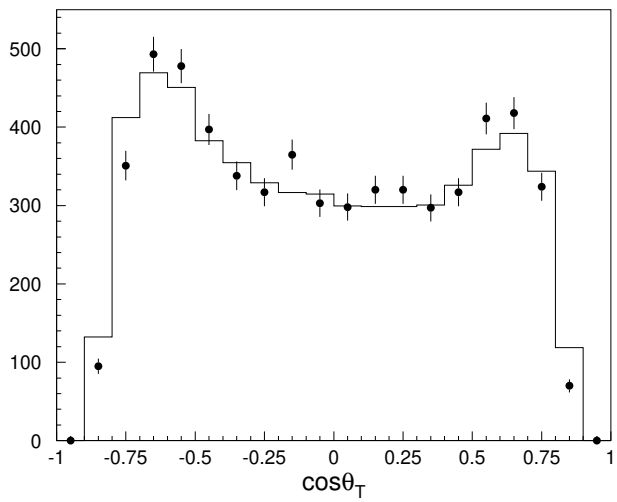

Figure 10: *Distributions of* $\cos\theta$ *for the thrust axis direction signed by the product* $(\delta Q \times P_e)$ *for data (points) and Monte Carlo (histograms) in the Charge Dipole analysis.*

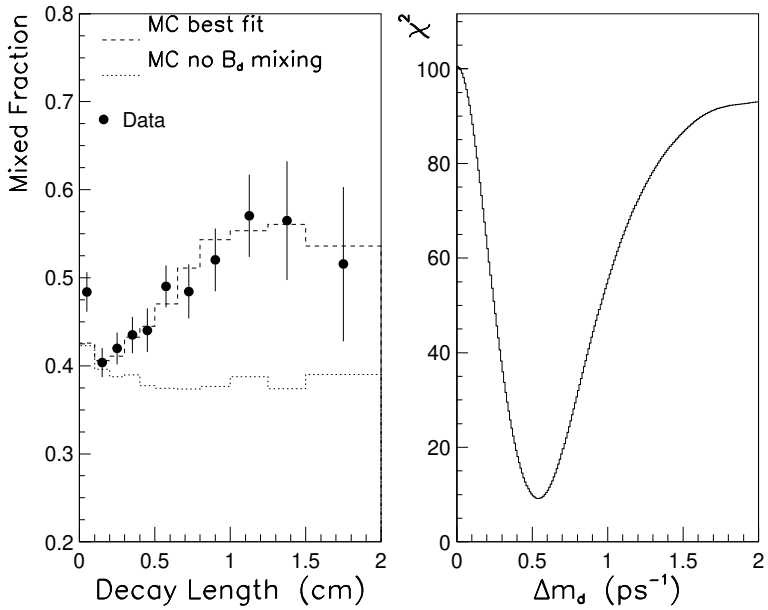

Figure 11: *Mixed fraction as a function of decay length for data (points) and best fit MC (dashed histogram) in the Charge Dipole analysis, also shown is the MC prediction without* B_d^0–$\overline{B_d^0}$ *mixing (dotted histogram). The* χ^2 *of the fit is shown on the right.*

shows a larger mixed fraction in the data than in the MC for $L < 1$ mm, indicating that the MC tag purity is overestimated in that decay length range by about 0.10. This effect is included in the study of systematic uncertainties.

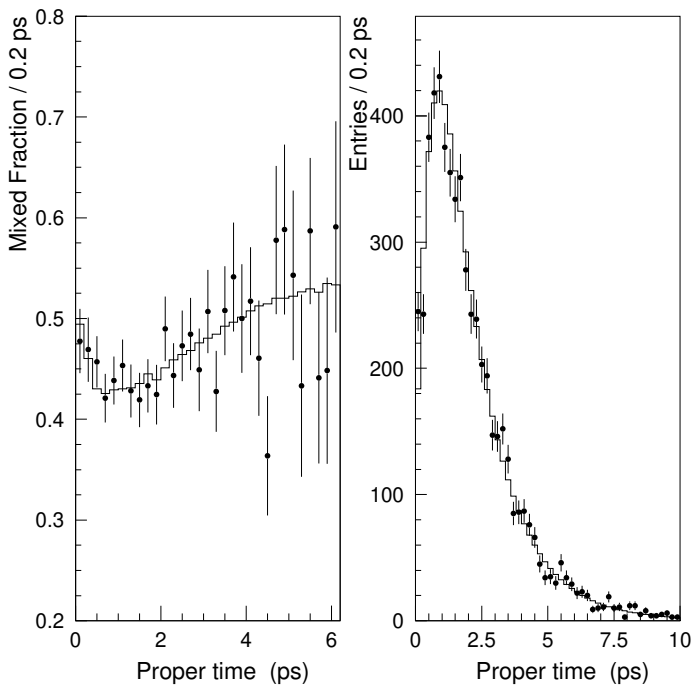

Figure 12: *Distributions of the fraction of decays tagged as "mixed" (left) and reconstructed proper time (right) for the data (points) and the likelihood function (histograms) in the Charge Dipole analysis.*

The reconstructed time distribution is shown in Fig. 12 along with the mixed fraction as a function of proper time (rather than decay length as in Fig. 11). The latter clearly shows the effect of degraded final state tag purity for decays at small proper time.

5.1 Likelihood Analysis

The B_s^0–$\overline{B_s^0}$ mixing fit is done in a way similar to that used for the lepton+D analysis. Slight differences are as follows: the decay length resolution σ_L does

not use the vertex fit and IP position measurement errors but is extracted from the overall decay length residual distributions in the simulation. Furthermore, σ_L is parameterized separately for decays with right and wrong charge dipole tags as it was found that the resolution is considerably higher for the correctly tagged decays (this is similar to differences in resolution between $(b \to l)$ and $(b \to c \to l)$ in the lepton+D analysis). For example, the decay length resolution for B_s^0 decays with right (wrong) charge dipole tag is parameterized by a sum of two Gaussians of widths $\sigma_{L1} = 131\ \mu$m (193 μm) and $\sigma_{L2} = 500\ \mu$m (761 μm), where the first Gaussian represents 60% of the decays. In addition, the decay length resolution is parameterized in three ranges of $|\cos\theta_T|$: 0.0 – 0.3, 0.3 – 0.6, and above 0.6, since the resolution decreases significantly as $|\cos\theta_T|$ increases.

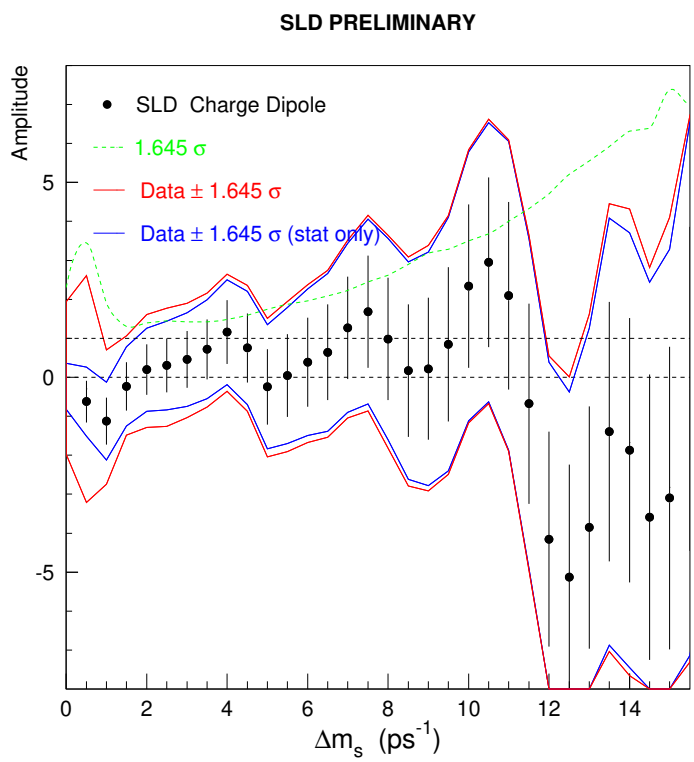

Figure 13: *Measured amplitude as a function of Δm_s in the Charge Dipole analysis.*

The result of the amplitude fit is displayed in Fig. 13. Systematic uncer-

Table 2: Measured values of the oscillation amplitude A with a breakdown of systematic uncertainties for several Δm_s values in the Charge Dipole analysis.

Δm_s	2 ps^{-1}	5 ps^{-1}	10 ps^{-1}
Measured amplitude A	0.194	-0.244	2.336
σ_A^{stat}	± 0.648	± 0.966	± 2.098
σ_A^{syst}	$^{+0.545}_{-0.646}$	$^{+0.441}_{-0.520}$	$^{+0.355}_{-0.377}$
$f_s = \mathcal{B}(b \to B_s^0)$	$^{-0.206}_{+0.306}$	$^{-0.168}_{+0.269}$	$^{-0.107}_{+0.253}$
$f_\Lambda = \mathcal{B}(b \to b\text{−baryon})$	$^{+0.016}_{-0.010}$	$^{+0.040}_{-0.009}$	$^{+0.063}_{-0.027}$
$udsc$ fraction	$^{+0.247}_{-0.197}$	$^{+0.211}_{-0.136}$	$^{+0.101}_{-0.004}$
decay length resolution	$^{+0.031}_{-0.018}$	$^{+0.041}_{+0.005}$	$^{+0.011}_{-0.007}$
boost resolution	$^{-0.003}_{-0.054}$	$^{+0.089}_{-0.116}$	$^{-0.254}_{-0.212}$
b-hadron lifetimes	$^{+0.012}_{-0.007}$	$^{+0.032}_{-0.000}$	$^{+0.016}_{-0.049}$
Δm_d	$^{-0.075}_{-0.043}$	$^{-0.057}_{-0.051}$	$^{-0.035}_{-0.058}$
initial state tag	$^{+0.120}_{-0.140}$	$^{+0.010}_{+0.024}$	$^{-0.066}_{+0.108}$
final state tag	$^{+0.355}_{-0.553}$	$^{+0.255}_{-0.452}$	$^{+0.189}_{-0.094}$

tainties are estimated as for the lepton+D analysis except for those affecting the final state tag. Here, uncertainties in the tag purity modeling are obtained by varying the final state correct tag probability by ± 0.05. In addition, a decrease of 0.08 in this probability was applied to the decays within $L < 1$ mm, to study the effect of the higher mixed fraction seen in the data (see Fig. 11). Dominant uncertainties are the B_s^0 production fraction in $Z^0 \to b\,\overline{b}$ events and the uncertainty in the final state tag purity, see Table 2.

6 Combination of the Analyses

The lepton+D and Charge Dipole analyses are combined taking into account correlated systematic errors. Figure 14 shows the measured amplitude as a function of Δm_s for the combination. As noted earlier, the measured values are consistent with $A = 0$ for the whole range of Δm_s up to 15 ps^{-1} and no evidence is found for a preferred value of the mixing frequency. The following

ranges of B_s^0–$\overline{B_s^0}$ oscillation frequencies are excluded at 95% C.L.: $\Delta m_s < 1.7$ ps^{-1} and $3.3 < \Delta m_s < 5.0$ ps^{-1}, i.e., the condition $A+1.645\sigma_A < 1$ is satisfied for those values. The combined sensitivity to set a 95% C.L. lower limit is found to be at a Δm_s value of 4.2 ps^{-1}. These results are preliminary.

It is worth noting that the overall sensitivity is expected to improve rapidly as the rest of the 1998 data and more analysis techniques are added.

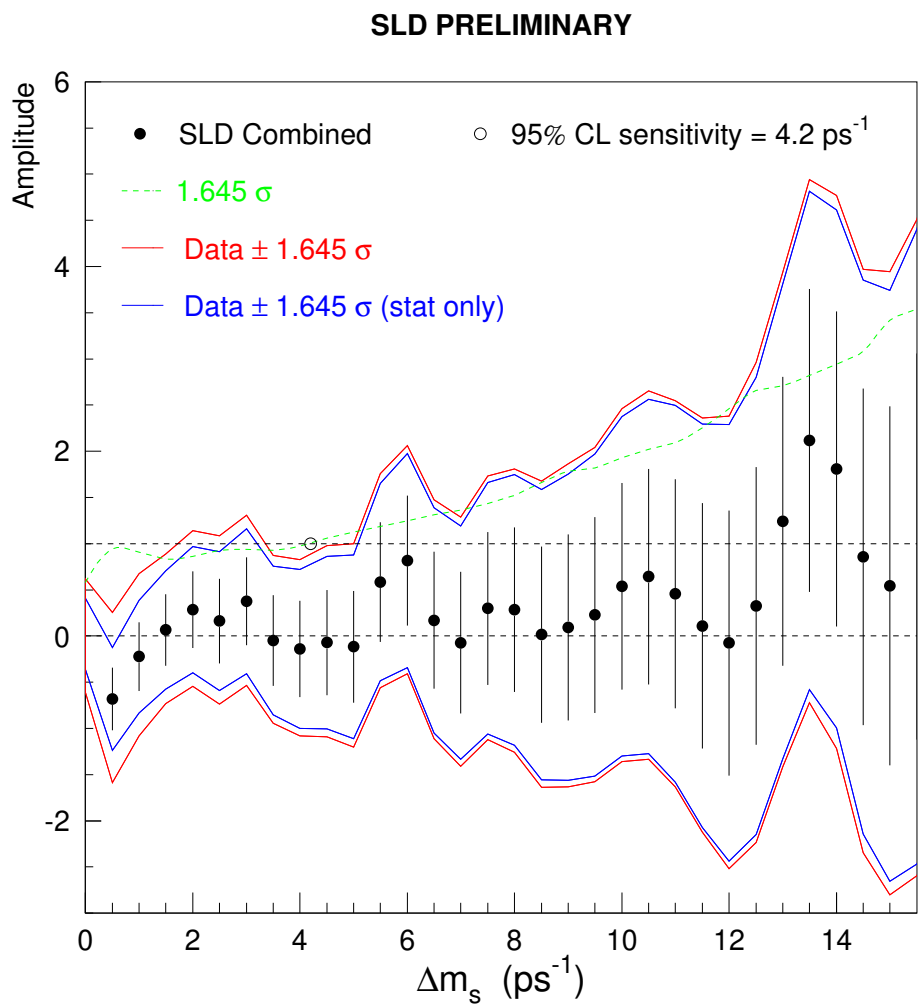

Figure 14: *Measured amplitude as a function of Δm_s for the lepton+D and Charge Dipole analyses combined.*

Acknowledgments

We thank the personnel of the SLAC accelerator department and the technical staffs of our collaborating institutions for their outstanding efforts.

References

[1] P. Paganini, F. Parodi, P. Roudeau, and A. Stocchi, *Measurements of the ρ and η Parameters of the V_{CKM} Matrix and Perspectives*, `hep-ph/9711261` and `hep-ph/9802289`.

[2] K. Abe *et al.*, Phys. Rev. **D53**, 1023 (1996).

[3] K. Abe *et al.*, Nucl. Inst. and Meth. **A400**, 287 (1997).

[4] T. Sjöstrand, Comp. Phys. Comm. **82**, 74 (1994).

[5] CLEO B decay model provided by P. Kim and the CLEO Collaboration.

[6] B. Barish *et al.*, Phys. Rev. Lett. **76**, 1570 (1996); H. Albrecht *et al.*, Z. Phys. **C58**, 191 (1993); H. Albrecht *et al.*, Z. Phys. **C62**, 371 (1994); P. Avery *et al.*, CLEO CONF 96-28, July 1996; L. Gibbons *et al.*, Phys. Rev. **D56**, 3783 (1997); T.E. Coan *et al.*, CLNS 97/1516; CLEO Collab., CLEO CONF 97-27, Aug. 1997; M. Zoeller, Ph.D. Thesis, SUNY Albany, 1994; X. Fu *et al.*, Phys. Rev. Lett. **79**, 3125 (1997); D. Gibaut *et al.*, Phys. Rev. **D53**, 4734 (1996).

[7] N. Isgur, D. Scora, B. Grinstein, and M.B. Wise, Phys. Rev. **D39**, 799 (1989).

[8] Particle Data Group, Phys. Rev. **D54**, Part I (1996).

[9] C. Peterson *et al.*, Phys. Rev. **D27**, 105 (1983).

[10] R. Brun *et al.*, Report No. CERN-DD/EE/84-1, 1989.

[11] D. J. Jackson, Nucl. Inst. and Meth. **A388**, 247 (1997).

[12] K. Abe *et al.* (SLD Collaboration), *Measurement of the B^+ and B^0 Lifetimes using Topological Vertexing at SLD*, SLAC-PUB-7868, July 1998, contributed paper # 180 to ICHEP98.

[13] K. Abe *et al.*, Phys. Rev. Lett. **80**, 660 (1998).

[14] K. Abe *et al.*, Phys. Rev. **D56**, 5310 (1997).

[15] H.-G. Moser and A. Roussarie, Nucl. Inst. and Meth. **A384**, 491 (1997).

[16] K. Abe *et al.*, *Preliminary Measurements of the Time Dependence of* $B_d^0 - \overline{B_d^0}$ *Mixing with Kaon and Charge Dipole Tags*, SLAC-PUB-7230, July 1996, contribution (PA08-027/028) to ICHEP96.

[17] LEP B Oscillations Working Group, *Combined Results on* B^0 *Oscillations: Results for Summer 1998 Conferences*, LEPBOSC 98/3, July 1998.

**List of Authors

K. Abe,[2] K. Abe,[19] T. Abe,[27] I.Adam,[27] T. Akagi,[27] N. J. Allen,[4] A. Arodzero,[20] W.W. Ash,[27] D. Aston,[27] K.G. Baird,[15] C. Baltay,[37] H.R. Band,[36] M.B. Barakat,[14] O. Bardon,[17] T.L. Barklow,[27] J.M. Bauer,[16] G. Bellodi,[21] R. Ben-David,[37] A.C. Benvenuti,[3] G.M. Bilei,[23] D. Bisello,[22] G. Blaylock,[15] J.R. Bogart,[27] B. Bolen,[16] G.R. Bower,[27] J. E. Brau,[20] M. Breidenbach,[27] W.M. Bugg,[30] D. Burke,[27] T.H. Burnett,[35] P.N. Burrows,[21] A. Calcaterra,[11] D.O. Caldwell,[32] D. Calloway,[27] B. Camanzi,[10] M. Carpinelli,[24] R. Cassell,[27] R. Castaldi,[24] A. Castro,[22] M. Cavalli-Sforza,[33] A. Chou,[27] E. Church,[35] H.O. Cohn,[30] J.A. Coller,[5] M.R. Convery,[27] V. Cook,[35] R. Cotton,[4] R.F. Cowan,[17] D.G. Coyne,[33] G. Crawford,[27] C.J.S. Damerell,[25] M. N. Danielson,[7] M. Daoudi,[27] N. de Groot,[27] R. Dell'Orso,[23] P.J. Dervan,[4] R. de Sangro,[11] M. Dima,[9] A. D'Oliveira,[6] D.N. Dong,[17] P.Y.C. Du,[30] R. Dubois,[27] B.I. Eisenstein,[12] V. Eschenburg,[16] E. Etzion,[36] S. Fahey,[7] D. Falciai,[11] C. Fan,[7] J.P. Fernandez,[33] M.J. Fero,[17] K.Flood,[15] R. Frey,[20] T. Gillman,[25] G. Gladding,[12] S. Gonzalez,[17] E.L. Hart,[30] J.L. Harton,[9] A. Hasan,[4] K. Hasuko,[31] S. J. Hedges,[5] S.S. Hertzbach,[15] M.D. Hildreth,[27] J. Huber,[20] M.E. Huffer,[27] E.W. Hughes,[27] X.Huynh,[27] H. Hwang,[20] M. Iwasaki,[20] D. J. Jackson,[25] P. Jacques,[26] J.A. Jaros,[27] Z.Y. Jiang,[27] A.S. Johnson,[27] J.R. Johnson,[36] R.A. Johnson,[6] T. Junk,[27] R. Kajikawa,[19] M. Kalelkar,[26] Y. Kamyshkov,[30] H.J. Kang,[26] I. Karliner,[12] H. Kawahara,[27] Y. D. Kim,[28] R. King,[27] M.E. King,[27] R.R. Kofler,[15] N.M. Krishna,[7] R.S. Kroeger,[16] M. Langston,[20] A. Lath,[17] D.W.G. Leith,[27] V. Lia,[17] C.-J. S. Lin,[27] X. Liu,[33] M.X. Liu,[37] M. Loreti,[22] A. Lu,[32] H.L. Lynch,[27] J. Ma,[35] G. Mancinelli,[26] S. Manly,[37] G. Mantovani,[23] T.W. Markiewicz,[27] T. Maruyama,[27] H. Masuda,[27] E. Mazzucato,[10] A.K. McKemey,[4] B.T. Meadows,[6] G. Menegatti,[10] R. Messner,[27] P.M. Mockett,[35] K.C. Moffeit,[27] T.B. Moore,[37] M.Morii,[27] D. Muller,[27] V.Murzin,[18] T. Nagamine,[31] S. Narita,[31] U. Nauenberg,[7] H. Neal,[27] M. Nussbaum,[6] N.Oishi,[19] D. Onoprienko,[30] L.S. Osborne,[17] R.S. Panvini,[34] H. Park,[20] C. H. Park,[29] T.J. Pavel,[27] I. Peruzzi,[11] M. Piccolo,[11] L. Piemontese,[10] E. Pieroni,[24] K.T. Pitts,[20] R.J. Plano,[26] R. Prepost,[36] C.Y. Prescott,[27] G.D. Punkar,[27] J. Quigley,[17] B.N. Ratcliff,[27] T.W. Reeves,[34] J. Reidy,[16]

P.L. Reinertsen,[33] P.E. Rensing,[27] L.S. Rochester,[27] P.C. Rowson,[8] J.J. Russell,[27] O.H. Saxton,[27] T. Schalk,[33] R.H. Schindler,[27] B.A. Schumm,[33] J. Schwiening,[27] S. Sen,[37] V.V. Serbo,[36] M.H. Shaevitz,[8] J.T. Shank,[5] G. Shapiro,[13] D.J. Sherden,[27] K. D. Shmakov,[30] C. Simopoulos,[27] N.B. Sinev,[20] S.R. Smith,[27] M. B. Smy,[9] J.A. Snyder,[37] H. Staengle,[9] A. Stahl,[27] P. Stamer,[26] R. Steiner,[1] H. Steiner,[13] M.G. Strauss,[15] D. Su,[27] F. Suekane,[31] A. Sugiyama,[19] S. Suzuki,[19] M. Swartz,[27] A. Szumilo,[35] T. Takahashi,[27] F.E. Taylor,[17] J. Thom,[27] E. Torrence,[17] N. K. Toumbas,[27] A.I. Trandafir,[15] J.D. Turk,[37] T. Usher,[27] C. Vannini,[24] J. Va'vra,[27] E. Vella,[27] J.P. Venuti,[34] R. Verdier,[17] P.G. Verdini,[24] S.R. Wagner,[27] D. L. Wagner,[7] A.P. Waite,[27] Walston, S.,[20] J.Wang,[27] C. Ward,[4] S.J. Watts,[4] A.W. Weidemann,[30] E. R. Weiss,[35] J.S. Whitaker,[5] S.L. White,[30] F.J. Wickens,[25] B. Williams,[7] D.C. Williams,[17] S.H. Williams,[27] S. Willocq,[27] R.J. Wilson,[9] W.J. Wisniewski,[27] J. L. Wittlin,[15] M. Woods,[27] G.B. Word,[34] T.R. Wright,[36] J. Wyss,[22] R.K. Yamamoto,[17] J.M. Yamartino,[17] X. Yang,[20] J. Yashima,[31] S.J. Yellin,[32] C.C. Young,[27] H. Yuta,[2] G. Zapalac,[36] R.W. Zdarko,[27] J. Zhou.[20]

(The SLD Collaboration)

[1] *Adelphi University, South Avenue- Garden City,NY 11530,*
[2] *Aomori University, 2-3-1 Kohata, Aomori City, 030 Japan,*
[3] *INFN Sezione di Bologna, Via Irnerio 46 I-40126 Bologna, Italy,*
[4] *Brunel University, Uxbridge, Middlesex - UB8 3PH United Kingdom,*
[5] *Boston University, 590 Commonwealth Ave. - Boston,MA 02215,*
[6] *University of Cincinnati, Cincinnati,OH 45221,*
[7] *University of Colorado, Campus Box 390 - Boulder,CO 80309,*
[8] *Columbia University, Nevis Laboratories P.O.Box 137 - Irvington,NY 10533,*
[9] *Colorado State University, Ft. Collins,CO 80523,*
[10] *INFN Sezione di Ferrara, Via Paradiso,12 - I-44100 Ferrara, Italy,*
[11] *Lab. Nazionali di Frascati, Casella Postale 13 I-00044 Frascati, Italy,*
[12] *University of Illinois, 1110 West Green St. Urbana,IL 61801,*
[13] *Lawrence Berkeley Laboratory, Dept.of Physics 50B-5211 University of California- Berkeley, CA 94720,*
[14] *Louisiana Technical University, Dept. of Physics, Ruston, LA 71272,*
[15] *University of Massachusetts, Amherst,MA 01003,*

[16] *University of Mississippi, University,MS 38677,*
[17] *Massachusetts Institute of Technology, 77 Massachusetts Avenue Cambridge, MA 02139,*
[18] *Moscow State University, Institute of Nuclear Physics 119899 Moscow, Russia,*
[19] *Nagoya University, Nagoya 464 Japan,*
[20] *University of Oregon, Department of Physics Eugene,OR 97403,*
[21] *Oxford University, Oxford, OX1 3RH, United Kingdom,*
[22] *Universita di Padova, Via F. Marzolo,8 I-35100 Padova, Italy,*
[23] *Universita di Perugia, Sezione INFN, Via A. Pascoli I-06100 Perugia, Italy,*
[24] *INFN, Sezione di Pisa, Via Livornese,582/AS Piero a Grado I-56010 Pisa, Italy,*
[25] *Rutherford Appleton Laboratory, Chiton,Didcot - Oxon OX11 0QX United Kingdom,*
[26] *Rutgers University, Serin Physics Labs Piscataway,NJ 08855-0849,*
[27] *Stanford Linear Accelerator Center, 2575 Sand Hill Road Menlo Park,CA 94025,*
[28] *Sogang University, Ricci Hall Seoul, Korea,*
[29] *Soongsil University, Dongjakgu Sangdo 5 dong 1-1 Seoul, Korea 156-743,*
[30] *University of Tennessee, 401 A.H. Nielsen Physics Blg. - Knoxville, Tennessee 37996-1200,*
[31] *Tohoku University, Bubble Chamber Lab. - Aramaki - Sendai 980, Japan,*
[32] *U.C. Santa Barbara, 3019 Broida Hall Santa Barbara,CA 93106,*
[33] *U.C. Santa Cruz, Santa Cruz,CA 95064,*
[34] *Vanderbilt University, Stevenson Center,Room 5333 P.O.Box 1807,Station B Nashville,TN 37235,*
[35] *University of Washington, Seattle,WA 98105,*
[36] *University of Wisconsin, 1150 University Avenue Madison,WS 53706,*
[37] *Yale University, 5th Floor Gibbs Lab. - P.O.Box 208121 - New Haven,CT 06520-8121.*